nature communications

Matters arising

https://doi.org/10.1038/s41467-023-39498-y

On the existence of collective interactions reinforcing the metal-ligand bond in organometallic compounds

Received: 28 November 2022

Accepted: 8 June 2023

Published online: 03 July 2023

Check for updates

Jordi Poater[1,2], Pascal Vermeeren[3], Trevor A. Hamlin[3], F. Matthias Bickelhaupt[3,4,5] ✉ & Miquel Solà[6] ✉

ARISING FROM S. Sowlati-Hashjin et al. *Nature Communications* https://doi.org/10.1038/s41467-022-29504-0 (2022)

Recently, Sowlati-Hashjin et al.[1] concluded that the nature of the Li–C chemical bond in $LiCF_3$ differs significantly from that in $LiCPh_3$ (Ph = phenyl). Whereas the Li–C bond of $LiCF_3$ is classified as a conventional two-center two-electron bond (exchange-correlation interaction collectivity index, $ICI_{XC} = 0.910$, $ICI_{XC} > 0.9$ and close to 1), that of $LiCPh_3$ is categorized as a collective bond ($ICI_{XC} = 0.393$). The authors claim that collective bonds take place in systems composed of MAR_3 (M = metal; A = C, B or Al; R = substituent) when M forms a stronger bond with the substituents R than with the central atom A. They claim the M–A interaction is either destabilizing or weakly stabilizing, whilst the 1,3-M•••R interactions are strongly stabilizing, but their method does not provide a causal mechanism that would demonstrate the correctness of this interpretation of the ICI_{XC} index. Here, we prove the opposite, namely, that the Li–CPh_3 bond is not reinforced or provided by collective interactions, but that it is weakened by 1,3-M•••R contacts, which reduce the bond overlap. On top of that, there is 1,3-M•••R closed-shell overlap that further reduces the stability through Pauli repulsion. Taken together, our results suggest that there is no need to define the collective interaction as a new type of chemical bond.

We analyze the Li–C bond in $LiCR_3$ (R = F, Ph) using quantitative Kohn-Sham molecular orbital (MO) theory in conjunction with the activation strain model (ASM) and a matching energy decomposition analysis (EDA)[2–4] at M06-2X/TZ2P[5] with the Amsterdam Density Functional (ADF)[6,7] program. We stress that our physical model that provides causal relationships and thus explanations is the MO model and not, as often incorrectly stated, EDA. The latter is a tool that quantifies features in the MO bonding mechanism. Additionally, we analyze the Li–C bond in the doublet ground state of $LiCR_2^{\bullet}$ and the triplet ground state of $LiCR^{\bullet\bullet}$ using the optimized geometry of the parent molecule (Supplementary Fig. 1).

Table 1 gathers the results of the ASM and EDA for the homolytic Li–CR_n (R = F, Ph; n = 1–3) bond cleavage into Li· + ·CR_n radicals[8,9]. The ΔE_{oi} component is the most important stabilizing contribution in the homolytic dissociation of $LiCF_3$, which is driven by the bonding overlap S and energy difference $\Delta\varepsilon$ between the SOMOs of Li· and ·CF_3 (Supplementary Figs. 2 and 3). In addition, there is only a weak donor–acceptor interaction between the lone pair on the F atoms and the SOMO and LUMO of Li (Supplementary Fig. 4). Thus, the Li–C bond behaves as a typical electron-pair bond between Li· and ·CF_3, and hence, is a polar covalent interaction. Interestingly, the Li–C bond becomes stronger going from $LiCF_3$ to $LiCF_2^{\bullet}$ to $LiCF^{\bullet\bullet}$, due to stabilization of the SOMO(·CF_n) because reducing the number of F substituents reduces antibonding overlap between the C $2p_z$ and F $2p_z$ atomic orbitals (Supplementary Figs. 2 and 3). At difference, ΔV_{elstat} slightly decreases from $LiCF_3$ to $LiCF^{\bullet\bullet}$, by only around 3 kcal mol^{-1}.

Moving to $LiCPh_3$, we find that the Li–C bond dissociation energy is around 20 kcal mol^{-1} less stabilizing than for $LiCF_3$ (Table 1). This weakening originates from the more destabilizing Pauli repulsion, due to the larger steric size and slightly shorter Li–R distance of R = Ph compared to R = F. For the same reason, ΔV_{elstat} becomes more stabilizing, leading to a Li–C in the $LiCPh_3$ system with a nearly balanced ratio between the electrostatic (ΔV_{elstat}) and covalent (ΔE_{oi}) contributions. The ΔE_{oi}, on the other hand, is similar to that of $LiCF_3$; whereas $LiCPh_3$ shows a weaker electron-pair bonding than $LiCF_3$, this is compensated by stronger donor–acceptor interactions (Supplementary Table 4 and Supplementary Figs. 5–8).

These data indicate that the nature of the Li–C bond is similar in $LiCF_3$ and $LiCPh_3$ and do not favor a classification of the Li–C bond as conventional in $LiCF_3$ *versus* collective in $LiCPh_3$. Additionally, if we had a collective bond in $LiCPh_3$, we should expect a reduction of the Li–C bond strength when going from $LiCPh_3$ to $LiCPh_2^{\bullet}$ to $LiCPh^{\bullet\bullet}$. We, in

[1]Departament de Química Inorgànica i Orgànica & Institut de Química Teòrica i Computacional (IQTCUB), Universitat de Barcelona, Martí i Franquès 1-11, 08028 Barcelona, Spain. [2]ICREA, Pg. Lluís Companys 23, 08010 Barcelona, Spain. [3]Department of Chemistry and Pharmaceutical Sciences, Amsterdam Institute of Molecular and Life Sciences (AIMMS), Vrije Universiteit Amsterdam, De Boelelaan 1083, 1081 HV Amsterdam, The Netherlands. [4]Institute of Molecules and Materials (IMM), Radboud University, Heyendaalseweg 135, 6525 AJ Nijmegen, The Netherlands. [5]Department of Chemical Sciences, University of Johannesburg, Auckland Park, Johannesburg 2006, South Africa. [6]Institut de Química Computacional i Catàlisi (IQCC) and Departament de Química, Universitat de Girona, C/ M. Aurèlia Capmany, 69, 17003 Girona, Catalonia, Spain. ✉e-mail: F.M.Bickelhaupt@vu.nl; miquel.sola@udg.edu

https://doi.org/10.1038/s41467-023-39498-y

Table 1 | Homolytic activation strain and energy decomposition analyses (in kcal mol^{-1}) of $LiCR_n$ (R = F, Ph; n = 1–3), singly-occupied molecular orbitals (SOMOs) energy difference ($\Delta\varepsilon$ in eV) and overlap integrals.[a]

Species	ΔE	ΔE_{strain}	ΔE_{int}	ΔE_{Pauli}	ΔV_{elstat}	ΔE_{oi}	$\Delta\varepsilon$	Overlap[b]
$LiCF_3$	−63.6	15.1	−78.6	46.6	−29.7	−95.5	4.8	0.317
$LiCF_2$•	−83.9	10.6	−94.6	35.1	−28.1	−101.6	6.3	0.322
LiCF••	−122.2	1.6	−123.8	21.8	−27.0	−118.6	8.7	0.330
$LiCPh_3$	−45.5	4.9	−50.4	157.1	−109.3	−98.2	1.1	0.071
$LiCPh_2$•	−43.0	9.3	−52.3	114.0	−83.2	−83.2	2.5	0.167
LiCPh••	−84.5	1.9	−86.4	68.7	−56.6	−98.5	5.1	0.229

[a]Computed at M06-2X/TZ2P. d(Li–C) = 1.997 and 1.980 Å for $LiCF_3$ and $LiCPh_3$, respectively. LiCF•• and LiCPh•• are in the triplet state, which corresponds to their valence state in the full parent molecule.
[b]Overlap integrals < SOMO(Li•) | SOMO(•CPh_x) > forming the Li–C pair bond. See also Supplementary Table 1 and Supplementary Figs. 13–16.

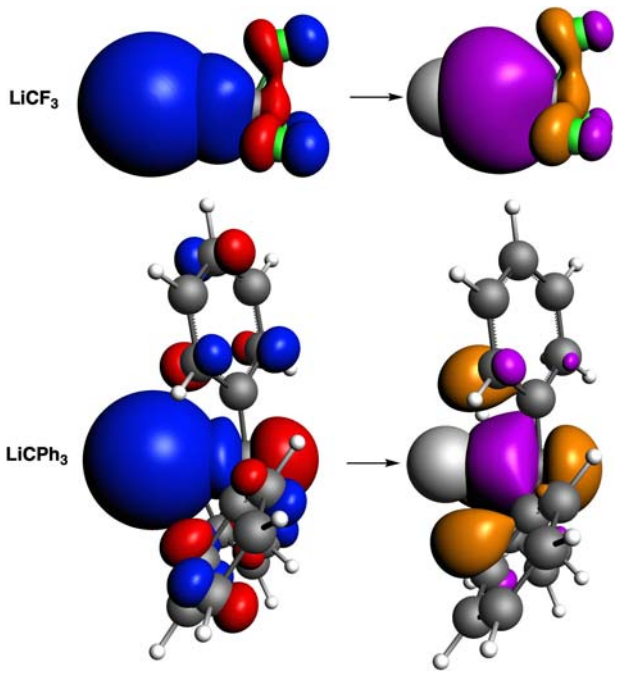

Fig. 1 | Overlap density between the two singly-occupied molecular orbitals (SOMOs) of $LiCF_3$ and $LiCPh_3$. Isosurfaces of the superposed SOMO of Li• and the SOMO of •CR_3 (R = F, Ph) to construct $LiCF_3$ and $LiCPh_3$ (left, isovalue = 0.05 a.u.). Red and blue isosurfaces represent positive and negative phases. Overlap density between the two SOMOs (right, isovalue = 0.001 a.u.). Purple and orange isosurfaces indicate in-phase and out-of-phase overlap, respectively. See also Supplementary Figs. 9–12.

fact, see the exact opposite, namely, the Li–C bond strength increases when going from $LiCPh_3$ to LiCPh••, mainly because of the reduced destabilizing Pauli repulsion due to the steric repulsion of the Ph groups, while the contribution of ΔE_{oi} to the Li–C interaction remains more or less constant from $LiCPh_3$ to LiCPh••.

Notably, the in-phase overlap (Fig. 1, in purple) between the SOMO of Li (2*s*) and the SOMO of CR_3 ($2p_z$ fragments) to form the Li–C bond is much larger for $LiCF_3$ than for $LiCPh_3$. At difference, the out-of-phase overlap (in orange) with the R groups is larger for the latter. Thus, the weaker Li–C interaction in $LiCPh_3$, despite the expected collective interactions that should make it stronger, is in part also due to the cancelation of bond overlap that reduces the bond strength instead of providing bonding. The addition of more substituents in contact with Li drives to the cancellation of bond overlap as evidenced by the decrease in overlap densities from $LiCPh_3$ to $LiCPh_2$• to LiCPh•• (Supplementary Fig. 12). In other words, the collectivity of contacts reduces the bond strength instead of generating extra stability. This cancellation effect can also be observed in the comparison between $LiCF_3$ discussed above to *i*-$LiCF_3$, which has also been considered to possess collective interactions (Supplementary Fig. 11). Thus, the collectivity of contacts reduces the bond strength and hence affords no additional stability. This latter statement is also supported by the computed EDA-NOCV deformation densities (Supplementary Fig. 18), which indicate similar orbital interactions in $LiCF_3$, *i*-$LiCF_3$, and $LiCPh_3$.

In conclusion, our quantitative MO and EDA study does not reveal any sign of collective interaction in $LiCPh_3$ that makes the Li–C interaction stronger, but, in fact, the opposite. The small ICI_{XC}, calculated as V_{XC}(Li–C)/V_{XC}(Li–{T}) where T stands for the set of all atoms of the system except the C directly attached to Li, of $LiCPh_3$ of Sowlati-Hashjin et al.[1] is likely the result of dividing a relatively low V_{XC}(Li–C), because of the high polarity of this bond, by a large number of small long-range V_{XC}(Li–C_{Ph}) and V_{XC}(Li–H_{Ph}) contributions. It does not reflect any special chemical bond in this species, let alone a strong through-space interaction between the Li and the phenyl groups that could indicate collective bonding. Our results show that the nature of the Li–C bond of $LiCPh_3$ does not differ significantly from that of $LiCF_3$, but only that the former has weaker electron-pair bonding, which is compensated by stronger donor–acceptor interactions. Finally, we have analyzed the inverted $LiCF_3$ cluster. Not unexpectedly, in this case, the ICI_{XC} is small, but this is simply the result of a low V_{XC}(Li–C) because of the large distance between Li and C and a large V_{XC}(Li–F) due to the short Li–F distance (Supplementary Fig. 1 and Supplementary Table 2). Lastly, we anyway do not see a need to rebrand collective bonding as a *new* flavor of the chemical bond. The concept has been invoked already in other cases and is therefore not novel[10,11].

Methods

All calculations were performed with the Amsterdam Density Functional (ADF) module of the AMS2021 software package at the M06-2X/TZ2P level of theory[5–7,12]. The geometry optimizations were carried out without symmetry constraints (Supplementary Table 5). Numerical Hessians were computed to characterize the optimized structures as minima (zero imaginary frequencies). Geometries for $LiCX_2$• and LiCX•• (X = F or Ph) were not allowed to relax but performed at the same geometry of $LiCX_3$ with the removal of either one (doublet state) or two X substituents (triplet state), respectively. $LiCX_2$• and LiCX•• were computed at their doublet or triplet state, respectively. For this latter, the singlet state has been proven to be higher in energy in all cases.

The Li–C interaction was analyzed within the framework of quantitative Kohn-Sham molecular orbital theory in combination with a quantitative activation strain model (ASM) and energy decomposition analysis (EDA) in the gas phase. Both homolytic and heterolytic breaking schemes of Li–C bond have been studied. For instance, in $LiCF_3$, we may have Li• (one unpaired alpha electron) and •CF_3 (one unpaired beta electron) fragments for the homolytic breaking. Or we may have Li^+ and $^-CF_3$ fragments in case of the heterolytic breaking.

Activation strain and energy decomposition analysis

For the activation strain model (ASM), the bond energy ΔE between two fragments is made up of two components[3,13]:

$$\triangle E = \triangle E_{strain} + \triangle E_{int} \quad (1)$$

Here, the strain energy ΔE_{strain} is the amount of energy required to deform the fragments from their equilibrium structure to the geometry that they acquire in the overall complex. The interaction energy

ΔE_{int} corresponds to the actual energy change when the geometrically deformed fragments are combined to form the overall complex.

We further analyze the interaction ΔE_{int} in the framework of the Kohn-Sham molecular orbital (MO) model, by dissecting it through our canonical energy decomposition analyses (EDA) into the electrostatic attraction, the Pauli repulsion and the (attractive) orbital interactions:

$$\triangle E_{int} = \triangle V_{elstat} + \triangle E_{Pauli} + \triangle E_{oi} \quad (2)$$

The term ΔV_{elstat} corresponds to the classical electrostatic interaction between the unperturbed charge distributions of the fragments in the geometry they possess in the complex. This term is usually attractive. The Pauli repulsion ΔE_{Pauli} between these fragments comprises the destabilizing interactions, associated with the Pauli principle for fermions, between occupied orbitals and is responsible for the steric repulsion. The orbital interaction ΔE_{oi} between these fragments in any MO model, and therefore also in Kohn-Sham theory, accounts for electron-pair bonding (the SOMO–SOMO interaction), charge transfer (empty/occupied orbital mixing between different fragments), and polarization (empty/occupied orbital mixing on one fragment due to the presence of another fragment). The orbital interaction energy ΔE_{oi} can be further decomposed into the contributions from each irreducible representation Γ of the interacting system. The use of M06-2X gives a term that cannot be decomposed, which is a correction term, such that the total orbital interaction is the correct one.

Voronoi deformation density (VDD) charge

The electron density distribution is analyzed by using the Voronoi deformation density (VDD) method for atomic charges[14]. The VDD atomic charge Q_A^{VDD} is computed as the (numerical) integral of the deformation density $\Delta\rho(\mathbf{r}) = \rho(\mathbf{r}) - \sum_B \rho_B(\mathbf{r})$ in the volume of the Voronoi cell of atom A [Eq. (3)]. The Voronoi cell of atom A is defined as the compartment of space bound by the bond midplanes on and perpendicular to all bond axes between nucleus A and its neighboring nuclei (cf. the Wigner-Seitz cells in crystals)[14].

$$Q_A^{VDD} = -\int_{\text{Voronoi cell of A}} \left[\rho(\mathbf{r}) - \sum_B \rho_B(\mathbf{r})\right] d\mathbf{r} \quad (3)$$

In Eq. (3), $\rho(\mathbf{r})$ is the electron density of the molecule and $\sum_B \rho_B(\mathbf{r})$ the superposition of atomic densities ρ_B of a fictitious promolecule without chemical interactions that is associated with the situation in which all atoms are neutral. The interpretation of the VDD charge Q_A^{VDD} is rather straightforward and transparent. Instead of measuring the amount of charge associated with a particular atom A, Q_A^{VDD} directly monitors how much charge flows, due to chemical interactions, out of ($Q_A^{VDD} > 0$) or into ($Q_A^{VDD} < 0$) the Voronoi cell of atom A, that is, the region of space that is closer to nucleus A than to any other nucleus.

ETS-NOCV calculations

The natural orbitals for chemical valence method (ETS-NOCV) have been computed at the same M06-2X/TZ2P level of theory. It allows one to visualize the alteration in the electronic structure of the interacting species, which is associated with bond formation. In particular, we have depicted the deformation densities, whose shapes provide a visualization of the associated pairwise orbital interactions[15].

Data availability

All data generated or analyzed during this study are included in this published article (and its supplementary information files).

References

1. Sowlati-Hashjin, S. et al. Collective interactions among organometallics are exotic bonds hidden on lab shelves. *Nat. Commun.* **13**, 2069 (2022).
2. Bickelhaupt, F. M. & Houk, K. N. Analyzing reaction rates with the distortion/interaction-activation strain model. *Angew. Chem. Int. Ed.* **56**, 10070–10086 (2017).
3. Bickelhaupt, F. M. & Baerends, E. J. in *Reviews in Computational Chemistry* (eds. Lipkowitz K. B. & Boyd D. B.). 1–86 (Wiley-VCH, 2000).
4. Frenking G. & Bickelhaupt F. M. in *The Chemical Bond*. (eds. Frenking, G. & Shaik, S.) 121–157 (Wiley, 2014).
5. Zhao, Y. & Truhlar, D. G. The M06 suite of density functionals for main group thermochemistry, thermochemical kinetics, noncovalent interactions, excited states, and transition elements: two new functionals and systematic testing of four M06-class functionals and 12 other functionals. *Theor. Chem. Acc.* **120**, 215–241 (2008).
6. te Velde, G. et al. Chemistry with ADF. *J. Comput. Chem.* **22**, 931–967 (2001).
7. Baerends E. J. et al. *ADF 2022.1, SCM, Theoretical Chemistry* (Vrije Universiteit, Amsterdam, The Netherlands, 2022).
8. Bickelhaupt, F. M., Solà, M. & Fonseca Guerra, C. Covalence in highly polar bonds. structure and bonding of methylalkalimetal oligomers $(CH_3M)_n$ (M = Li - Rb, n = 1,4). *J. Chem. Theory Comput.* **2**, 965–980 (2006).
9. Bickelhaupt, F. M. et al. Clarifying notes on the bonding analysis adopted by the energy decomposition analysis. *Phys. Chem. Chem. Phys.* **24**, 15726–15735 (2022).
10. Goesten, M. G., Hoffmann, R., Bickelhaupt, F. M. & Hensen, E. J. M. Eight-coordinate fluoride in a silicate double-four-ring. *Proc. Nat. Acad. Sci. USA* **114**, 828–833 (2017).
11. Jašík, J., Gerlich, D. & Roithová, J. Probing isomers of the benzene dication in a low-temperature trap. *J. Am. Chem. Soc.* **136**, 2960–2962 (2014).
12. van Lenthe, E. & Baerends, E. J. Optimized Slater-type basis sets for the elements 1–118. *J. Comput. Chem.* **24**, 1142–1156 (2003).
13. Vermeeren, P., van der Lubbe, S. C. C., Fonseca Guerra, C., Bickelhaupt, F. M. & Hamlin, T. A. Understanding chemical reactivity using the activation strain model. *Nat. Protoc.* **15**, 649–667 (2020).
14. Fonseca Guerra, C., Handgraaf, J.-W., Baerends, E. J. & Bickelhaupt, F. M. Voronoi deformation density (VDD) charges: assessment of the Mulliken, Bader, Hirshfeld, Weinhold, and VDD methods for charge analysis. *J. Comput. Chem.* **25**, 189–210 (2004).
15. Michalak, A., DeKock, R. L. & Ziegler, T. Bond multiplicity in transition-metal complexes: applications of two-electron valence indices. *J. Phys. Chem. A* **112**, 7256–7263 (2008).

Acknowledgements

The authors thank the Spanish Ministerio de Ciencia e Innovación (projects PID2020-13711GB-I00, PID-2019-106830GB-I00, and CEX2021-001202-M), the Generalitat de Catalunya (projects 2021SGR623 and 2021SGR442), the Netherlands Organization for Scientific Research (NWO), and the Holland Research School of Molecular Chemistry (HRSMC) for a fellowship to M.S. for visiting the TheoCheM group at Vrije Universiteit Amsterdam.

Author contributions

F.M.B. and M.S. conceived the research idea. J.P. did the calculations. J.P., P.V., T.A.H., F.M.B., and M.S. analyzed the data and wrote the manuscript.

Competing interests
The authors declare no competing interests.

Additional information
Supplementary information The online version contains supplementary material available at https://doi.org/10.1038/s41467-023-39498-y.

Correspondence and requests for materials should be addressed to F. Matthias Bickelhaupt or Miquel Solà.